

Preprocessing noise in finite-size quantum key distribution

Gabriele Staffieri,^{1,2} Giuseppe D’Ambruoso,^{2,3,4} Giovanni Scala,^{2,4} and Cosmo Lupo^{1,2,4}

¹*Dipartimento Interateneo di Fisica, Università di Bari, 70126 Bari, Italy*

²*INFN, Sezione di Bari, 70126 Bari, Italy*

³*Dipartimento di Meccanica, Matematica e Management, Politecnico di Bari, 70125 Bari, Italy*

⁴*Dipartimento Interateneo di Fisica, Politecnico di Bari, 70126 Bari, Italy*

It is known that preprocessing noise may boost quantum key distribution by expanding the range of values of tolerated noise. For BB84, adding trusted noise may allow the generation of secret keys even for qubit error rate (QBER) beyond the 11% threshold in the asymptotic regime. Here we study the effect of preprocessing noise in the finite-size regime where only a limited number of signals are exchanged between Alice and Bob. We compute tight numerical lower bounds in terms of the sandwiched Rényi entropy of order α , optimized via two-step Frank–Wolfe algorithm, in the presence of a trusted flipping probability q . We find that trusted noise improves the key rate only for a finite interval of α , from the $\alpha \rightarrow 1$ limit up to $\alpha \simeq 1.4$. By optimizing on the value of α , we determine finite-size key rates for different values of the QBER, observing enhancement due to trusted noise both in asymptotic and finite-size regime. Finally, we determine the maximum tolerable QBER as a function of the block size.

I. INTRODUCTION

Quantum key distribution (QKD) enables two distant users, commonly called Alice and Bob, to establish a shared secret key with information-theoretic security based on the principles of quantum physics and suitable additional assumptions, even against adversaries with unlimited quantum computational power. Nowadays security analyses typically adopt composable frameworks that takes into account finite-size correction, using one-shot entropic quantities and their asymptotic behaviors [1, 2].

In discrete-variable (DV) protocols, information is encoding in discrete degrees of freedom of the quantum electromagnetic fields, and measurements are usually performed on complementary bases. Among the various DV protocols, the BB84 is the most well-known example [3], which has played a fundamental role for the development of experiments and security proofs [4]. Composable security proofs offer general bounds on the finite-size key rates and clarify the impact of classical preprocessing and postprocessing steps on the security [5, 6]. One important example is *trusted local randomization*, where one party flips each bit of the sifted key with a given probability before information reconciliation. This preprocessing is often referred to as *trusted-noise injection*; in this way, one of the legitimate user adds local randomness which is inaccessible to a possible eavesdropper. In the asymptotic limit where an unbounded number of signals is exchanged, this technique has been proven to increase the secret-key rate, especially when the quantum bit error rate (QBER) is high, as shown in early studies [7, 8].

Recent work on finite-size security indicates that using Rényi entropies can lead to tighter key-rate bounds for practical block lengths [9]. In DV QKD, several frameworks based on Rényi entropy and entropy accumulation have been developed and applied—for example, in decoy-state protocols [10, 11]. Furthermore, similar techniques have also been explored in continuous-variable

(CV) settings, including CV QKD with discrete modulation under Gaussian attacks [12–14]. As a matter of fact, sandwiched Rényi entropies provide a direct and tight quantification of the secret-key generation rate without passing through the procedure of min-entropy smoothing [9, 15].

These developments motivate a deeper analysis on the role of trusted noise in the finite-size regime. Here we develop this analysis in terms of sandwiched Rényi entropies. In contrast with other entropic quantities, such as the von Neumann entropy and the min-entropy, Rényi-based bounds respond differently to noise levels and introduce the Rényi order α as an additional optimization parameter. This may affect the trade-off between the privacy gain from trusted noise and the increased information leakage from error reconciliation. As a consequence, the expected key-rate enhancement may no longer hold in all regimes.

In this work, we analyze the security of BB84, with trusted preprocessing noise, against collective (i.i.d.) attacks, in the finite-size regime. First, we identify the range of values of the Rényi order α for which trusted noise remains beneficial, through a comparison of the key rates with and without optimally tuned randomization. Second, for fixed values of the QBER, we determine the maximum achievable finite-size key-rate by jointly optimizing over the randomization parameter (the bit-flip probability q) and the Rényi order. Third, we investigate the maximum tolerable values of the QBER as a function of the block size. We evaluate the required entropic quantities numerically by recasting the problem into a form suitable for efficient convex optimization and performing a systematic outer optimization over both parameters. Methodologically, our numerical evaluation builds on the reliable two-step framework for key rate computation introduced in [16, 17], which exploits the Frank–Wolfe algorithm [18]. Adapting this approach to our setting requires handling an objective function of fundamentally different nature, since the privacy term

is expressed through sandwiched Rényi entropies rather than von Neumann entropies. In particular, the Frank–Wolfe iterations require explicit analytical gradients of the Rényi-based objective. While related gradient formulas have appeared in prior work for a simplified objective function depending on a single optimization variable [19], our setting requires a more general treatment. Indeed, we work with a fully variational Rényi entropy objective function that retains the auxiliary optimization, such that the Frank–Wolfe updates must be driven by gradients with respect to *two* coupled variables, rather than a single variable.

II. METHODOLOGY

A. Protocol model (BB84 with trusted local randomization)

To assess the security of the protocol, we consider the entanglement-based (EB) representation of the BB84 protocol, with the introduction of trusted preprocessing noise. Furthermore, we work under the assumption of collective attacks, where each quantum signal transmission from Alice to Bob is subject to i.i.d. noise. Before proceeding, we briefly recall a high-level description of the protocol:

1. *Preparation and transmission:* Alice prepares n identical maximally entangled qubit pairs $|\Phi^+\rangle_{AA'} = (|0\rangle_A|0\rangle_{A'} + |1\rangle_A|1\rangle_{A'})/\sqrt{2}$. She keeps qubit A and sends qubit A' to Bob.
2. *Measurement:* in each round, Alice and Bob measure in randomly chosen $\mathbb{Z} = \{|0\rangle, |1\rangle\}$ or $\mathbb{X} = \{|+\rangle, |-\rangle\}$ basis.
3. *Sifting:* they publicly announce the bases and keep only matched-basis rounds, obtaining m sifted bits out of n transmissions.
4. *Trusted local randomization:* before information reconciliation, Bob flips each sifted bit independently with probability q (hence introducing trusted noise).
5. *Information reconciliation:* in reverse reconciliation Bob reveals ℓ_{leak} bits of syndrome information.
6. *Privacy amplification:* a two-universal hash function extracts an ℓ -bit key from the reconciled strings.

Under the assumption of collective attacks, each signal transmission is described by an isometry $U_{A' \rightarrow BE}$ mapping Alice qubit A' into Bob qubit B and the environment E . The latter is without loss of generality prepared in a given state $|\phi\rangle_E$. The tri-partite state shared by Alice, Bob, and the environment, after step 1. of the protocol is

$$|\Theta\rangle_{ABE} = (\mathbb{I}_A \otimes U_{A' \rightarrow BE}) |\Phi^+\rangle_{AA'} |\phi\rangle_E. \quad (1)$$

The bipartite state shared by Alice and Bob after each transmission is $\rho_{AB} = \text{tr}_E(|\Theta\rangle\langle\Theta|)$. For collective attacks, the n -round state is the tensor power, $\rho_{A^n B^n} = \rho_{AB}^{\otimes n}$, where $A^n = A_1 \cdots A_n$ and $B^n = B_1 \cdots B_n$. The channel induced by $U_{A' \rightarrow BE}$ is determined by the adversary (denoted Eve) who controls and monitors the environment, and is unknown to the legitimate parties.

Let Z denote the random variable representing Bob's classical bit produced by his measurement in the \mathbb{Z} basis. Trusted noise is modeled as a local, random bit-flip,

$$Z \mapsto Y_1 = Z \oplus F, \quad F \sim \text{Bern}(q). \quad (2)$$

Equivalently, trusted randomization can be absorbed into the very definition of Bob's measurement. This measurement is then characterized by the POVM elements

$$\Lambda_0 = (1 - q)Z_0 + qZ_1, \quad (3)$$

$$\Lambda_1 = (1 - q)Z_1 + qZ_0, \quad (4)$$

where Z_j ($j = 0, 1$) are the \mathbb{Z} eigenprojectors.

Following Ref. [16], we introduce the *key map* \mathcal{G} associated to such a measurement. Its action on the state ρ_{AB} is

$$\mathcal{G}(\rho_{AB}) = \sum_{j=0,1} M_j \rho_{AB} M_j^\dagger, \quad (5)$$

with

$$M_j = \mathbb{I}_A \otimes \sqrt{\Lambda_j} \otimes |j\rangle_{Y_1}, \quad (6)$$

where the states $|j\rangle_{Y_1}$ encode the measurement outputs, i.e. the classical variable Y_1 .

The analogous construction can be introduced for Bob's measurement in the \mathbb{X} basis. For simplicity, here we assume that the QBER is the same in both bases, $Q_{\mathbb{Z}} = Q_{\mathbb{X}} = p$, where

$$Q_{\mathbb{X}} = \text{tr} \left[\Pi_X^{\text{err}} \rho_{AB} \right], \quad Q_{\mathbb{Z}} = \text{tr} \left[\Pi_Z^{\text{err}} \rho_{AB} \right], \quad (7)$$

being

$$\Pi_X^{\text{err}} = |+-\rangle_{AB} \langle +-| + |-+\rangle_{AB} \langle -+| \quad (8)$$

$$\Pi_Z^{\text{err}} = |01\rangle_{AB} \langle 01| + |10\rangle_{AB} \langle 10| \quad (9)$$

the projectors on the error events.

In order to assess the security of the protocol, it is convenient to introduce the isometry

$$V_{Y_1 \rightarrow Y Y_1} = \sum_{j=0,1} |j\rangle_Y \otimes |j\rangle_{Y_1} \langle j|_{Y_1} \quad (10)$$

(which satisfies the identity $V^\dagger V = \mathbb{I}_{Y_1}$). Formally, this creates a copy of Y_1 into an auxiliary register Y . Including this latter isometry, we can write a five-partite pure state

$$\rho_{ABYY_1E} = (V \otimes \mathbb{I}_E) \mathcal{G}(\rho_{ABE}) (V^\dagger \otimes \mathbb{I}_E). \quad (11)$$

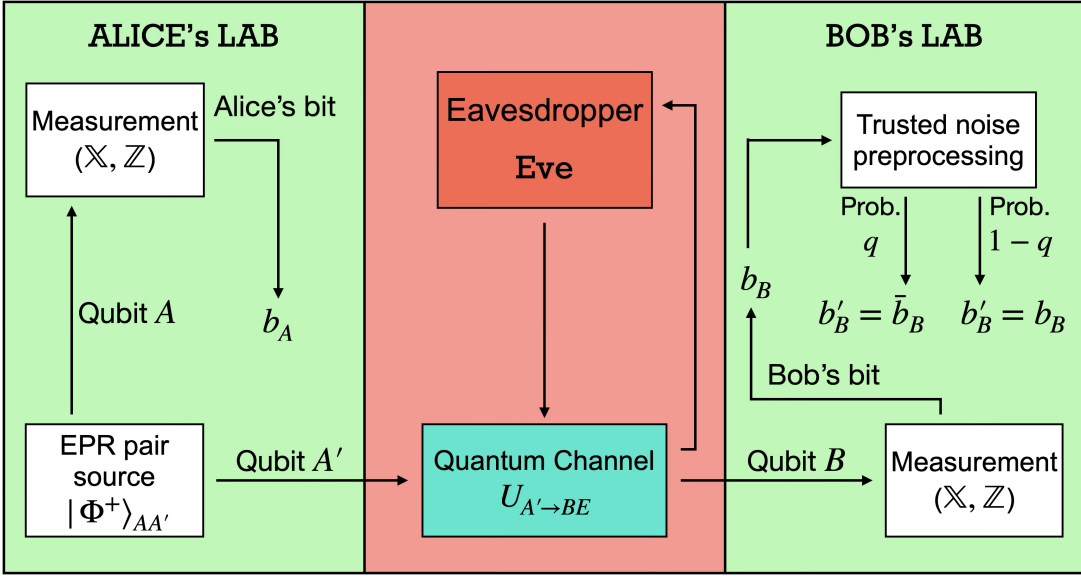


FIG. 1: Schematic of BB84 protocol with trusted noise preprocessing, in the entanglement-based representation. Alice and Bob's classical bits obtained through qubit measurements are indicated as b_A and b_B respectively. The symbol b'_B indicates Bob's bit after trusted bit flip.

We conclude this section noticing that the operation of partial trace, when applied on the auxiliary system Y , leaves the system in a state that is classical on system Y_1 . We have

$$\text{tr}_Y(\rho_{ABYY_1E}) = \mathcal{Z}(\mathcal{G}(\rho_{ABE})), \quad (12)$$

where \mathcal{Z} is the pinching map, which fully dephases the register Y_1 :

$$\mathcal{Z}(\mathcal{G}(\rho_{ABE})) = \sum_{j=0,1} |j\rangle_{Y_1} \langle j| \mathcal{G}(\rho_{ABE}) |j\rangle_{Y_1} \langle j|. \quad (13)$$

B. Secret-key rate and Rényi-divergence formulation

After sifting, Alice and Bob hold two highly correlated m -bit strings; we denote Bob's raw key as Y^m . The leftover-hash lemma, based on Rényi entropy [9], bounds the number ℓ of bits that can be extracted from Y^m such that Eve has little or no information about them. If

$$\ell \leq \tilde{H}_\alpha^\uparrow(Y^m|E^m) - g_\epsilon(\alpha) =: \ell_\epsilon(\alpha), \quad (14)$$

then one can extract a secret key of ℓ bits with security parameter ϵ . The above bound holds for any $\alpha \in (1, 2]$, where

$$g_\epsilon(\alpha) = \frac{\alpha}{\alpha-1} \log\left(\frac{1}{\epsilon}\right) - 2 \quad (15)$$

(we put $\log \equiv \log_2$), and $\tilde{H}_\alpha^\uparrow(A|B)$ denotes the optimized sandwiched Rényi conditional entropy,

$$\tilde{H}_\alpha^\uparrow(A|B)_\rho = \sup_{\sigma_B} \frac{1}{1-\alpha} \log \text{tr} \left[\left(\sigma_B^{\frac{1-\alpha}{2\alpha}} \rho_{AB} \sigma_B^{\frac{1-\alpha}{2\alpha}} \right)^\alpha \right], \quad (16)$$

(we put $\sigma_B = \mathbb{I}_A \otimes \sigma_B$).

It is convenient to recall the definition of the sandwiched Rényi divergence

$$\tilde{D}_\alpha(\rho||\omega) := \frac{1}{\alpha-1} \log \text{tr} \left[\left(\omega^{\frac{1-\alpha}{2\alpha}} \rho \omega^{\frac{1-\alpha}{2\alpha}} \right)^\alpha \right], \quad (17)$$

and its relation to the conditional entropy,

$$\tilde{H}_\alpha^\uparrow(A|B)_\rho = -\inf_{\sigma_B} \tilde{D}_\alpha(\rho_{AB} || \mathbb{I}_A \otimes \sigma_B). \quad (18)$$

As a figure of merit, here we focus on the following estimate for the finite-size, composable secret-key rate per sifted bit:

$$r_\epsilon = \frac{1}{m} (\ell_\epsilon(\alpha) - \ell_{\text{leak}}), \quad (19)$$

where ℓ_{leak} denotes the number of bits that Bob sends to Alice, through a public channel, to implement error correction. For our model, noise in the channel is a combination of untrusted and trusted bit-flip errors. Therefore, we put

$$\ell_{\text{leak}} = m h_2(s), \quad s = p(1-q) + (1-p)q, \quad (20)$$

where s is the *effective* QBER after trusted local randomization and $h_2(\cdot)$ is the binary Shannon entropy: $h_2(t) = -t \log t - (1-t) \log(1-t)$. Using the duality

relation between sandwiched Rényi entropies [20], and within the framework collective attacks, we obtain

$$\tilde{H}_\alpha^\uparrow(Y^m|E^m) = -m \tilde{H}_\beta^\uparrow(Y|ABY_1), \quad \beta = \frac{\alpha}{2\alpha - 1}, \quad (21)$$

which holds true since $\rho_{ABY_1E}^{\otimes m}$ is a pure state and is a tensor power. Moreover, the conditional entropy on the right-hand side admits a divergence representation directly in terms of the key map and pinching map introduced in the previous section [13]:

$$-\tilde{H}_\beta^\uparrow(Y|ABY_1) = \inf_{\sigma_{ABY_1}} \tilde{D}_\beta \left(\mathcal{G}(\rho_{AB}) \parallel \mathcal{Z}(\sigma_{ABY_1}) \right). \quad (22)$$

Accordingly, for given $(m, p, q, \alpha, \epsilon)$, we express the key rate as the Rényi divergence minus reconciliation and finite-size corrections ($\beta = \alpha/(2\alpha - 1)$):

$$r_\epsilon(m, \alpha, p, q) = \inf_{\sigma_{ABY_1}} \tilde{D}_\beta \left(\mathcal{G}(\rho_{AB}) \parallel \mathcal{Z}(\sigma_{ABY_1}) \right) - h_2(s) - \frac{g_\epsilon(\alpha)}{m}. \quad (23)$$

For later numerical optimization it is also useful to introduce the corresponding (unoptimized) objective function at fixed σ_{ABY_1} :

$$f_\epsilon(m, \alpha, p, q; \rho_{AB}, \sigma_{ABY_1}) := \tilde{D}_\beta \left(\mathcal{G}(\rho_{AB}) \parallel \mathcal{Z}(\sigma_{ABY_1}) \right) - h_2(s) - \frac{g_\epsilon(\alpha)}{m}. \quad (24)$$

C. Numerical methods

The best lower bound on the secret-key rate is returned by the overall optimization

$$\max_{q, \alpha} \min_{\rho_{AB}, \sigma_{ABY_1}}^* f(m, \alpha, p, q; \rho_{AB}, \sigma_{ABY_1}), \quad (25)$$

where \min^* denotes the *reliable* two-step numerical procedure of Ref. [16], adapted to our Rényi divergence objective. In the inner minimization, the optimization variables are the density operators ρ_{AB} and σ_{ABY_1} , with the additional constraint that $\rho_A = \mathbb{I}/2$. The value of the QBER (we assume symmetric QBER, $Q_Z = Q_X = p$) imposes two further linear constraints on ρ_{AB} . For given (m, p, q, α) , we optimize the sandwiched Rényi divergence and then combine it with the reconciliation and finite-size penalties, cf. Eq. (23). Following [16], the inner minimization \min^* is implemented with a Frank–Wolfe (FW) method over the feasible (convex) sets, where each FW step requires the gradient of the objective function with respect to the optimization variables. In our setting the objective function depends on *two* coupled vari-

ables, hence the FW direction is determined by the block-gradient $\nabla = \nabla_\rho \oplus \nabla_\sigma$, where

$$\nabla_\rho D_\beta \left(\mathcal{G}(\rho_{AB}) \parallel \mathcal{Z}(\sigma_{ABY_1}) \right) = \frac{(\ln 2)^{-1}}{\beta - 1} \mathcal{G}^\dagger \left(\frac{\chi_2}{Q_\beta(X\|Y)} \right) \quad (26)$$

$$\nabla_\sigma D_\beta \left(\mathcal{G}(\rho_{AB}) \parallel \mathcal{Z}(\sigma_{ABY_1}) \right) = \frac{(\ln 2)^{-1}}{\beta - 1} \mathcal{Z}^\dagger \left(\frac{\chi_1 + \chi_3}{Q_\beta(X\|Y)} \right) \quad (27)$$

with the notations

$$X = \mathcal{G}(\rho_{AB}), \quad Y = \mathcal{Z}(\sigma_{ABY_1}), \quad (28)$$

$$\mu = \frac{1 - \beta}{2\beta}, \quad \Xi = Y^\mu X Y^\mu, \quad Q_\beta(X\|Y) = \text{tr}[\Xi^\beta],$$

$$D_\beta(X\|Y) = \frac{1}{\beta - 1} \log(Q_\beta(X\|Y)). \quad (29)$$

and

$$\chi_1 = \beta \mathcal{T}_\mu^Y(A_1), \quad \chi_2 = \beta Y^\mu \Xi^{\beta-1} Y^\mu, \quad \chi_3 = \beta \mathcal{T}_\mu^Y(A_3), \quad (30)$$

with $A_1 = X Y^\mu \Xi^{\beta-1}$, $A_3 = \Xi^{\beta-1} Y^\mu X$, and $\mathcal{T}_\mu^Y(\cdot)$ the Fréchet-derivative map of Y^μ , defined by $\mathcal{T}_\mu^Y(\Delta Y) = \partial_{\Delta Y} Y^\mu$. (detailed calculation in Appendix A).

Finally, `minimize_scalar` from `scipy` has been used to find the optimal q , while a coarse-grained grid search has been exploited for finding the optimal Rényi orders.

III. RESULTS

In this section we present our results assessing the effect of the preprocessing noise on comparable security in the finite-size regime. First, we determine in which interval of values of α adding trusted noise improves the security of the protocol. To this end, we compute,

$$\Delta r(\alpha) = \max_p |r_\epsilon(\alpha, p, q^*) - r_\epsilon(\alpha, p)|, \quad (31)$$

where q^* is the optimal value of the trusted noise parameter that maximizes the key rate, and $r_\epsilon(\alpha, p) = r_\epsilon(\alpha, p, q = 0)$ is the key rate computed in absence of trusted local randomization; throughout this work we will assume $\epsilon = 10^{-10}$. We remark that the finite-size correction terms vanish in taking the difference between the two rates, thus this analysis is independent of the block-size m and on the security parameter ϵ . In taking the maximum *w.r.t.* eavesdropper's disturbance parameter p , we identify the values of p in which trusted bit flipping is beneficial.

In Fig. 2, the above quantifier is plotted against the Rényi order α . We observe that when $\alpha \rightarrow 1$ one obtains the highest gain from local randomization. In particular, this happens when $p \rightarrow 0.11$, which is the well-known

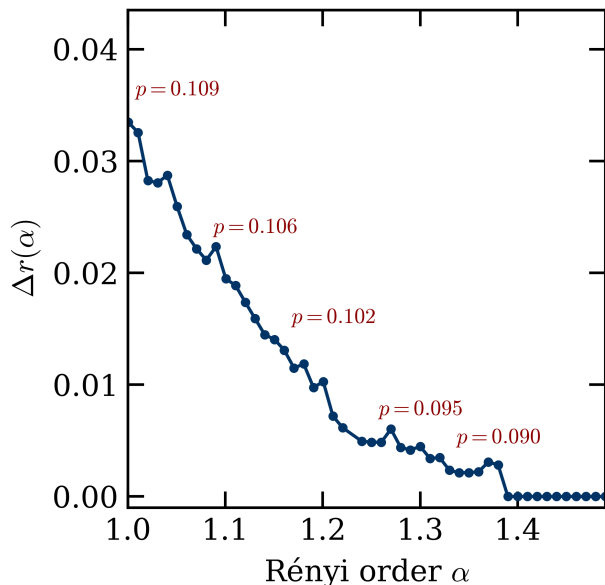


FIG. 2: Largest absolute difference between secret-key rates with optimal trusted noise level $r(\alpha, p, q^*)$ and without trusted randomization procedure $r(\alpha, p, q = 0)$, as in Eq. (31), plotted vs the Rényi order α . The level p of external noise at which Δr is found is displayed above the data points.

threshold value for for BB84 in absence of preprocessing noise [4]. As α increases, the gain diminishes, while the *best* external disturbance value p usually maintains values around $0.10 \lesssim p \lesssim 0.11$. This fact expresses one key feature: when trusted noise is beneficial, the most significant improvement of the key rate is always manifest at high QBER values. Finally, for $\alpha \gtrsim 1.4$, the addition of trusted bit flipping ceases to improve the key rate, as $q^* = 0$ for any observed adversarial disturbance p . (As we show in Appendix B, it is easy to verify that the in the limit $\alpha \rightarrow \infty$ preprocessing noise is never beneficial).

The heat map in Fig. 3 shows the trend of the optimal value of the trusted noise $q^*(\alpha, p)$, as a function of α and p . Here we restrict the domain of (α, p) in order to consider only non-vanishing key-rate values. As we could expect from the analysis of $\Delta r(\alpha)$, for small values of Eve’s disturbance, $p \leq 0.09$, the optimal level of trusted randomization is nearly zero, as $q^* < 0.01$. This is true for all values of the Rényi order parameter between $1 \lesssim \alpha \lesssim 1.2$. The trend changes when $p \gtrsim 0.10$. In particular at $p \simeq 0.11$, the impact of the Rényi order becomes significant, as for $1 \lesssim \alpha \lesssim 1.1$ we find $0.069 \lesssim q^* \lesssim 0.35$. Clearly, we observe q^* increasing as α gets larger, until the secret-key rate vanishes.

In Fig. 4 we show the best finite-size secret-key rate estimates (optimized over the Rényi order α) versus the sifted block length, for fixed values of Eve’s induced QBER p . The optimal values of the Rényi parameter are denoted as α^* . For each value of p we compare the

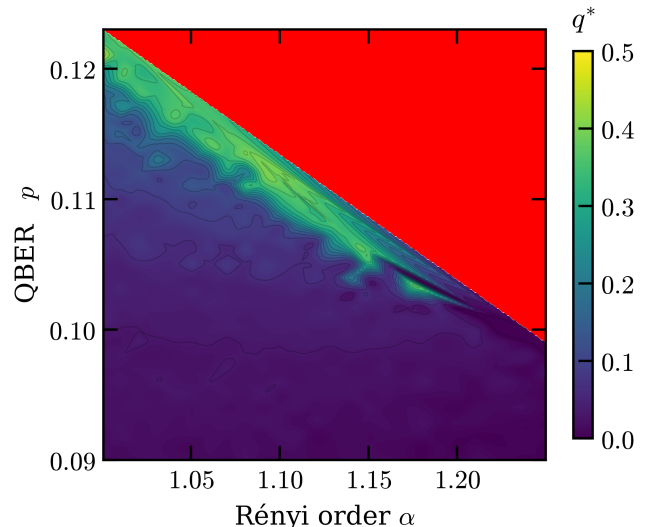


FIG. 3: Optimal trusted noise level $q^*(\alpha, p)$, as a function of the intrinsic eavesdropper’s noise p and Rényi order α . The domain (α, p) is restricted to those points for which $r(\alpha, p, q^*) > 0$; the forbidden domain is colored in red. The optimal trusted flipping probability grows as $p > 0.10$ for every value of α considered.

key rates obtained with optimally tuned trusted noise and without trusted noise, fixing the security parameter at $\epsilon = 10^{-10}$. We find that for $p \lesssim 0.09$ the two rate estimates essentially coincide, and trusted noise becomes actually beneficial only for $p \gtrsim 0.10$. For $p = 0.10$, Fig. 4 indicates that, for relatively small block sizes, preprocessing is required to achieve non-zero key rate. In the region beyond $m = 10^6$, the enhancement due to preprocessing is nearly independent on the block length. We found that the optimal trusted noise level lies in the interval $0.007 \lesssim q^* \lesssim 0.074$, and the optimal Rényi orders are, almost everywhere, in the interval $1 < \alpha^* \lesssim 1.06$. For $p = 0.11$, we observe that trusted local randomization yields a substantial improvement in the key rate. Most notably, trusted noise reduces, by several orders of magnitude, the minimum block length required to extract secret keys. We note that secret keys are obtained even for block lengths $m < 10^5$ in correspondence to an optimal flipping probability $q^* \simeq 0.098$. By contrast, without trusted noise, there is no secrecy for block sizes below 10^{11} . The optimal noise value decreases slightly as m grows, reaching $q^* \simeq 0.077$. The optimal value of the Rényi order is within the interval $1.01 \lesssim \alpha^* \lesssim 1.05$ for $m \lesssim 10^6$, and tends to $\alpha = 1$ asymptotically, as expected. Finally, in every QBER region such that $p > 0.11$, secrecy can be attained only with the assistance of trusted noise. As an example, we show the key rate for $p = 0.1238$. We observe that a non-zero key rate is achieved for $m = 2 \cdot 10^{11}$, and the asymptotic rate is nearly reached around $m \simeq 10^{13}$. The optimal flipping probability is

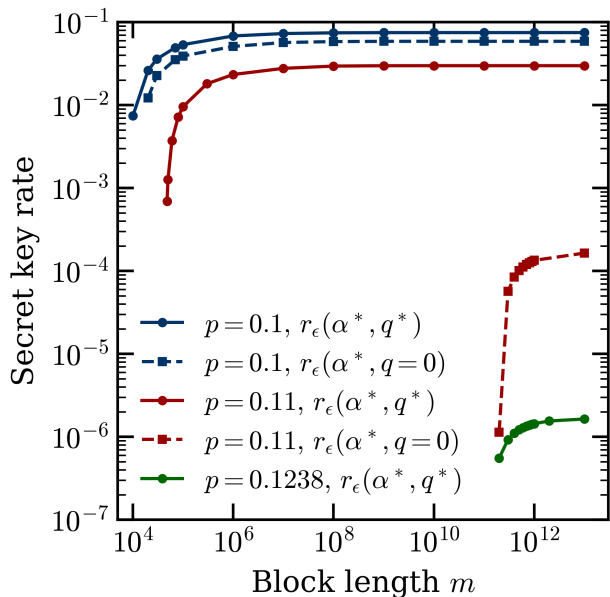


FIG. 4: Key rates at finite block size, following the optimization over the Rényi order α . We compare the key rate without trusted noise, and the key rate achieved with the optimal value of the trusted noise parameter q , with $\epsilon = 10^{-10}$. The optimal value of q and α are denoted q^* and α^* . Different lines refer to different values of the eavesdropper’s disturbance: $p = 0.10$; 0.11 ; 0.1238 . The security parameter is fixed at $\epsilon = 10^{-10}$. As the QBER increases, adding trusted noise becomes more beneficial, both in terms of absolute value of the secret-key rate value and in terms of minimum block length required for non-zero key generation.

always found around $q \simeq 0.37$ and the optimal Rényi parameter is very close to 1. We remark that no significant key rate is observed as $p \geq 0.124$, which is in agreement with the results of Renner *et al.* [5].

Finally, we determine the maximum tolerable QBER level, denoted p_{\max} , within the finite-block-length region $m \geq 10^3$, both with and without trusted noise, again with $\epsilon = 10^{-10}$. Figure 5 shows that preprocessing becomes more beneficial with increasing block size. Already around $m = 10^4$, the presence of trusted noise allows us to obtain non-zero key rate up to $p = 0.10$. By contrast, BB84 in absence of preprocessing cannot endure any QBER $p > 0.09$. For larger block lengths, trusted local randomization always guarantees higher QBER tolerance. Asymptotically, we recover the expected values, $p_{\max} = 0.124$ and $p_{\max} = 0.11$, respectively with and without trusted noise.

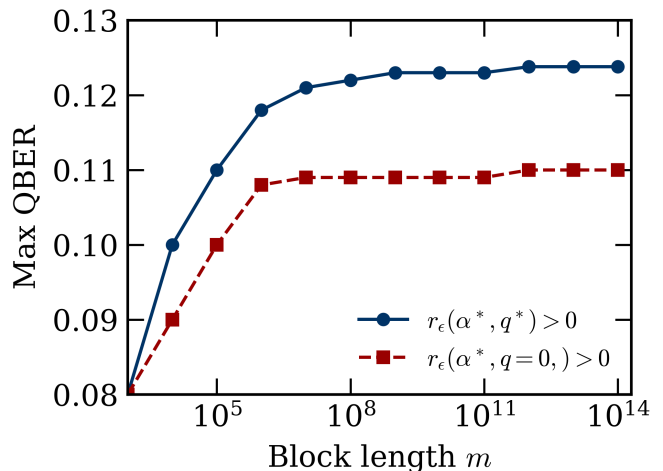


FIG. 5: Maximum tolerable QBER plotted vs the sifted block length m . The two lines compare the QBER threshold, with optimal trusted noise and without trusted noise. The security parameter is fixed at $\epsilon = 10^{-10}$. Up to $m = 10^3$, trusted noise does not enhance the QBER tolerance. Trusted noise becomes beneficial for $m \geq 10^4$. The asymptotic, known values, of $p_{\max} = 0.11$ and $p_{\max} = 0.124$ are retrieved for large block sizes.

IV. CONCLUSIONS

Preprocessing such as the injection of trusted noise is known to enhance the performance of QKD protocols, especially in terms tolerated QBER. This phenomenon has been extensively studied in the asymptotic limit in the number of channel uses [5–8]. Here we have focused on the finite-size regime, where statistical fluctuations need to be properly accounted for. Our composable security analysis, developed under the assumption of collective attacks, is based on sandwiched Rényi divergences [9, 19]. Throughout the work we have compared the key rates achieved with optimal level of trusted noise with those achieved without preprocessing, by varying the value of the Rényi order, the QBER, and in a wide range of block lengths, fixing the security parameter ϵ .

First, we have found that the enhancement which stems from trusted local randomization is observed only in a limited range of values of the Rényi order beyond $\alpha = 1$. This implies that key-rate estimators based on the min-entropy (obtained in the limit that $\alpha \rightarrow \infty$) are unaffected by trusted noise injection. This result can be obtained by direct calculations, as shown in Appendix B. This especially affects the finite-size regime, since the optimal Rényi order grows significantly when the block length becomes very small [13]. Second, we have shown that trusted noise becomes relevant when the QBER level reaches high values, which in general does not allow a non-zero key rate for small block sizes. It follows that trusted noise fails to provide any security advantage in

the regime of extremely small block sizes, when the standard BB84 protocol also fails. For example, for block size of 10^3 , the maximum tolerated QBER remains 0.08 in both scenarios, as the high value of the Rényi order required for such short blocks nullify the benefits of preprocessing. Nevertheless, preprocessing remains beneficial for larger block length. For example, for 10^4 sifted signals, trusted randomization allows for non-zero key rates up to QBER $p = 0.10$, whereas the standard protocol fails for $p > 0.09$. Beyond this threshold, preprocessing not only significantly reduces the minimum block size required for key extraction, but also provides a consistent absolute increase in the secret-key rate (see Fig. 4).

As for the numerical implementation, the two-step Frank-Wolfe framework manages to deal finely with the optimization of a high computational demanding objective function, as the *full variational* sandwiched Rényi divergence. However, the algorithm encounters some difficulties in computing Rényi entropies with an order α too close to 1, as should be expected. Some computational noise is also observed for higher values of α , this being the reason behind our choice of performing a coarse-grained optimization over α , rather than using `minimize.scalar`.

In terms of applications, our analysis may be extended to the framework of *Device-Independent* QKD [21–24]. Furthermore, tighter estimates on the key rates may be obtained using the latest leftover-hash lemma [25], which introduces measured smooth entropies and a novel Hermitian smoothing technique. This approach allows for smoothing over non-positive operators, providing a more precise one-shot characterization of privacy amplification and recovering the sharpest achievability results currently available.

The data that support the findings of this article are openly available [26].

ACKNOWLEDGMENTS

This work has received support by the European Union’s Horizon Europe research and innovation programme under the Project “Quantum Secure Networks Partnership” (QSNP, Grant Agreement No. 101114043), and by INFN through the project “QUANTUM”.

Appendix A: Derivation of the gradient for the sandwiched Rényi divergence

Here we derive the relation for the gradients ∇_ρ and ∇_σ which were shown in Eqs. (26)-(27). Here the derivation follows a similar strategy to that of Ref. [19], but extends it to the present setting where the objective functional depends on two distinct variables, ρ and σ , rather than on

a single optimization variable. We consider the objective

$$D_\beta(X||Y) = \frac{1}{\beta-1} \log(Q), \quad Q \equiv Q_\beta(X||Y) = \text{tr}(\Xi^\beta); \quad (\text{A1})$$

where we recall: $X = \mathcal{G}(\rho_{AB})$, $Y = \mathcal{Z}(\sigma_{ABY_1})$, $\Xi = Y^\mu X Y^\mu$, $\mu = (1-\beta)/2\beta$. Throughout this section we will denote with $\partial_{\Delta X}$ the directional derivative in such a way that $\forall \Delta X = \Delta X^\dagger$, [27]

$$\partial_{\Delta X} F(X) = \left. \frac{d}{dt} F(X + t\Delta X) \right|_{t=0} = \text{tr}((\nabla_X F)\Delta X). \quad (\text{A2})$$

We aim to compute the gradient *w.r.t.* ρ_{AB} . To do that, let us start from what follows. We need to fix Y and choose a *direction* ΔX , then we have

$$\partial_{\Delta X} \Xi = Y^\mu \Delta X Y^\mu. \quad (\text{A3})$$

Thus

$$\begin{aligned} \partial_{\Delta X} Q &= \beta \text{tr}(\Xi^{\beta-1} \partial_{\Delta X} \Xi) = \beta \text{tr}(\Xi^{\beta-1} Y^\mu \Delta X Y^\mu) \\ &= \beta \text{tr}(Y^\mu \Xi^{\beta-1} Y^\mu \Delta X) = \text{tr}(\chi_2 \Delta X), \end{aligned} \quad (\text{A4})$$

where we used cyclicity of the trace and $\chi_2 = \beta Y^\mu \Xi^{\beta-1} Y^\mu$. Hence the directional derivative of the Rényi divergence along ΔX is

$$\begin{aligned} \partial_{\Delta X} D_\beta(X||Y) &= \frac{1}{(\beta-1) \ln 2} \frac{1}{Q} \partial_{\Delta X} Q \\ &= \frac{1}{(\beta-1) \ln 2} \text{tr} \left(\frac{\chi_2}{Q} \Delta X \right). \end{aligned} \quad (\text{A5})$$

From Riesz lemma (A2), we can identify

$$\nabla_X D_\beta(X||Y) = \frac{1}{(\beta-1) \ln 2} \frac{\chi_2}{Q} \quad (\text{A6})$$

Finally we observe that $X = \mathcal{G}(\rho_{AB}) \implies \Delta X = \mathcal{G}(\Delta\rho)$ in such a way that

$$\begin{aligned} \partial_{\Delta\rho} D_\beta(\mathcal{G}(\rho)||Y) &= \text{tr}[(\nabla_X D_\beta) \mathcal{G}(\Delta\rho)] \\ &= \text{tr}[\mathcal{G}^\dagger(\nabla_X D_\beta) \Delta\rho], \end{aligned} \quad (\text{A7})$$

hence

$$\begin{aligned} \nabla_\rho D_\beta(\mathcal{G}(\rho_{AB})||\mathcal{Z}(\sigma_{ABY_1})) &= \mathcal{G}^\dagger(\nabla_X D_\beta(X||Y)) \\ &= \frac{1}{(\beta-1) \ln 2} \mathcal{G}^\dagger \left(\frac{\chi_2}{Q_\beta(X||Y)} \right). \end{aligned} \quad (\text{A8})$$

Now we compute the gradient *w.r.t.* σ_{ABY_1} . We fix X and consider a direction ΔY , and consider the Fréchet derivative of Y^μ in the integral representation [28]

$$\partial_{\Delta Y} Y^\mu = L(\mu) \int_0^\infty (Y+s)^{-1} \Delta Y (Y+s)^{-1} s^\mu ds, \quad (\text{A9})$$

with $L(\mu) = \frac{\sin(\pi\mu)}{\pi}$. Define the linear map

$$\mathcal{T}_\mu^Y(\Delta Y) := \partial_{\Delta Y} Y^\mu. \quad (\text{A10})$$

Then

$$\partial_{\Delta Y} \Xi = \mathcal{T}_\mu^Y(\Delta Y) X Y^\mu + Y^\mu X \mathcal{T}_\mu^Y(\Delta Y). \quad (\text{A11})$$

in such a way that

$$\begin{aligned} \partial_{\Delta Y} Q &= \beta \operatorname{tr}(\Xi^{\beta-1} \partial_{\Delta Y} \Xi) \\ &= \beta \operatorname{tr}(\Xi^{\beta-1} \mathcal{T}_\mu^Y(\Delta Y) X Y^\mu) + \beta \operatorname{tr}(\Xi^{\beta-1} Y^\mu X \mathcal{T}_\mu^Y(\Delta Y)) \\ &= \beta \operatorname{tr}(X Y^\mu \Xi^{\beta-1} \mathcal{T}_\mu^Y(\Delta Y)) + \beta \operatorname{tr}(\Xi^{\beta-1} Y^\mu X \mathcal{T}_\mu^Y(\Delta Y)). \end{aligned} \quad (\text{A12})$$

We next use the self-adjointness induced by (A9): for any A, B ,

$$\operatorname{tr}(A \mathcal{T}_\mu^Y(B)) = \operatorname{tr}(\mathcal{T}_\mu^Y(A) B), \quad (\text{A13})$$

which follows by inserting (A9) and using cyclicity of the trace. Setting

$$A_1 = X Y^\mu \Xi^{\beta-1}, \quad A_3 = \Xi^{\beta-1} Y^\mu X, \quad (\text{A14})$$

we can rewrite (A12) as

$$\begin{aligned} \partial_{\Delta Y} Q &= \beta \operatorname{tr}(A_1 \mathcal{T}_\mu^Y(\Delta Y)) + \beta \operatorname{tr}(A_3 \mathcal{T}_\mu^Y(\Delta Y)) \\ &= \operatorname{tr}\left(\beta(\mathcal{T}_\mu^Y(A_1) + \mathcal{T}_\mu^Y(A_3)) \Delta Y\right), \end{aligned} \quad (\text{A15})$$

where (A13) is applied term-wise. Therefore,

$$\begin{aligned} \partial_{\Delta Y} D_\beta(X\|Y) &= \frac{1}{(\beta-1) \ln 2} \frac{1}{Q} \partial_{\Delta Y} Q \\ &= \frac{1}{(\beta-1) \ln 2} \operatorname{tr}\left(\frac{\beta(\mathcal{T}_\mu^Y(A_1) + \mathcal{T}_\mu^Y(A_3))}{Q} \Delta Y\right) \\ &= \frac{1}{(\beta-1) \ln 2} \left(\frac{\chi_1 + \chi_3}{Q} \Delta Y\right) \end{aligned} \quad (\text{A16})$$

having set $\chi_1 = \beta \mathcal{T}_\mu^Y(A_1)$ and $\chi_3 = \beta \mathcal{T}_\mu^Y(A_3)$. Comparing (A16) with (A2), we identify

$$\nabla_Y D_\beta(X\|Y) = \frac{1}{(\beta-1) \ln 2} \frac{\chi_1 + \chi_3}{Q}. \quad (\text{A17})$$

Finally, $Y = \mathcal{Z}(\sigma_{ABY_1})$ implies $\Delta Y = \mathcal{Z}(\Delta\sigma)$, so

$$\begin{aligned} \partial_{\Delta\sigma} D_\beta(X\|\mathcal{Z}(\sigma)) &= \operatorname{tr}((\nabla_Y D_\beta) \mathcal{Z}(\Delta\sigma)) \\ &= \operatorname{tr}(\mathcal{Z}^\dagger(\nabla_Y D_\beta) \Delta\sigma). \end{aligned} \quad (\text{A18})$$

Hence

$$\begin{aligned} \nabla_\sigma D_\beta(\mathcal{G}(\rho_{AB})\|\mathcal{Z}(\sigma_{ABY_1})) &= \mathcal{Z}^\dagger(\nabla_Y D_\beta(X\|Y)) \\ &= \frac{1}{(\beta-1) \ln 2} \mathcal{Z}\left(\frac{\chi_1 + \chi_3}{Q_\beta(X\|Y)}\right) \end{aligned} \quad (\text{A19})$$

which holds since for a pinching map $\mathcal{Z}^\dagger = \mathcal{Z}$.

Appendix B: Effect of trusted noise on min-entropy ($\alpha \rightarrow \infty$) secret-key rate

Conditional min-entropy can be obtained from conditional sandwiched Rényi entropy taking the limit $\alpha \rightarrow \infty$ [29]:

$$\tilde{H}_{\min}^\dagger(A|B) = \lim_{\alpha \rightarrow \infty} \tilde{H}_\alpha^\dagger(A|B) \quad (\text{B1})$$

$$= \sup_{\sigma_B} -\log \left\| \sigma_B^{-\frac{1}{2}} \rho_{AB} \sigma_B^{-\frac{1}{2}} \right\|_\infty \quad (\text{B2})$$

This entropic quantity has the fundamental operational meaning of a *guessing probability* [30]

$$\tilde{H}_{\min}^\dagger(Y|E) = -\log P_g^{(0)}(Y|E) \quad (\text{B3})$$

being $P_g^{(0)}(Y|E)$ the probability for an eavesdropper to guess the correct value of the random variable Y , having access to some side information available in the quantum system E . Now it is worth noting that the guessing probability has a simple analytical expression for BB84 protocol with symmetric QBER [31–33]

$$P_g^{(0)}(Y|E) = \frac{1}{2} + \sqrt{p(1-p)} \quad (\text{B4})$$

with $p = Q_Z = Q_X$. Through leftover-hash lemma [34] the asymptotic secret-key rate under collective attacks can be bound by [33]:

$$r_{\min} \leq \tilde{H}_{\min}^\dagger(Y|E) - \gamma h_2(p) \quad (\text{B5})$$

$$= -\log P_g^{(0)}(Y|E) - \gamma h_2(p) \quad (\text{B6})$$

In this particular case, we consider error correction efficiency $\gamma > 1$, to be exhaustive. Now we observe that trusted noise alters Eve's guessing probability through a multiplicative factor $(1-2q)$, being q Bob's flipping probability

$$P_g^{(q)}(Y|E) = \frac{1}{2} + (1-2q)\sqrt{p(1-p)} \quad (\text{B7})$$

Hence, if trusted local randomization has to be taken into account, the bound on the secret-key rate turns into

$$r_{\min}(q) \leq -\log P_g^{(q)}(Y|E) - \gamma h_2(s(p, q)) \quad (\text{B8})$$

where $s(p, q) = p+q-2pq$ is the *observed* QBER. Here we want to show that, for the secret-key rate estimator considered, adding trusted noise does not provide an advantage; mathematically this is equivalent to show that when $r_{\min} > 0$, it is monotonically decreasing in $q \in [0, \frac{1}{2}]$.

a. Claim. On the physically relevant domain (*i.e.*, where the guessing probability bound is defined and $s(p, q) \leq \frac{1}{2}$), whenever $r_{\min}(q) > 0$ one has

$$r'_{\min}(q) \leq 0. \quad (\text{B9})$$

mathematically this statement translates into

$$\forall q \in [0, \frac{1}{2}] \text{ s.t. } r_{\min}(q) \geq 0 : \quad r'_{\min}(q) \leq 0 \quad (\text{B10})$$

b. Proof. First of all we set $t = \sqrt{p(1-p)}$ and $A(q) = \frac{1}{2} + (1-2q)t$; then the first and second derivative of $r_{\min}(q)$ read

$$r'_{\min}(q) = \frac{2t}{A(q) \ln 2} - \gamma(1-2p) \log \frac{1-s(q)}{s(q)} \quad (\text{B11})$$

$$r''_{\min}(q) = \frac{4t^2}{A(q)^2 \ln 2} + \frac{\gamma(1-2p)^2}{\ln 2} \frac{1}{s(q)[1-s(q)]} \quad (\text{B12})$$

It is easy to see that $\forall p, q \in [0, \frac{1}{2}] : r''_{\min}(q) > 0$, then $r_{\min}(q)$ is strictly convex in q everywhere in the physical domain. Moreover at the upper boundary:

$$\begin{aligned} r_{\min}\left(\frac{1}{2}\right) &= 1 - \gamma \leq 0, \\ r'_{\min}\left(\frac{1}{2}\right) &= \frac{4\sqrt{p(1-p)}}{\ln 2} > 0 \quad (0 < p < \frac{1}{2}). \end{aligned} \quad (\text{B13})$$

Since r_{\min} is convex and $r_{\min}(\frac{1}{2}) \leq 0$ with $r'_{\min}(\frac{1}{2}) > 0$, any region where $r_{\min}(q) > 0$ must lie to the left of the (at most single) zero of r'_{\min} . Let us indicate q_0 the unique root of r'_{\min} if it exists. The point $q = q_0$ is a minimum for r_{\min} , then in $[q_0, \frac{1}{2}]$ r_{\min} is increasing and bounded above by $r_{\min}(\frac{1}{2}) \leq 0$, hence $r_{\min} \leq 0$ there; therefore all points with $r_{\min} > 0$ lie in $[0, q_0)$ where $r'_{\min} \leq 0$. If r'_{\min} had no zero and were nonnegative throughout, r_{\min} would be increasing on $[0, \frac{1}{2}]$ and thus $r_{\min}(\frac{1}{2}) \geq r_{\min}(0)$, contradicting $r_{\min}(\frac{1}{2}) \leq 0$ when $r_{\min}(0) > 0$. Hence, in every point with $r_{\min}(q) > 0$ one necessarily has $r'_{\min}(q) \leq 0$. \square

-
- [1] R. Renner, Security of quantum key distribution, *International Journal of Quantum Information* **6**, 1 (2008).
- [2] M. Tomamichel, *Quantum information processing with finite resources: mathematical foundations*, Vol. 5 (Springer, 2015).
- [3] C. H. Bennett and G. Brassard, Quantum cryptography: Public key distribution and coin tossing, *Theoretical computer science* **560**, 7 (2014).
- [4] P. W. Shor and J. Preskill, Simple proof of security of the bb84 quantum key distribution protocol, *Physical review letters* **85**, 441 (2000).
- [5] R. Renner, N. Gisin, and B. Kraus, Information-theoretic security proof for quantum-key-distribution protocols, *Physical Review A—Atomic, Molecular, and Optical Physics* **72**, 012332 (2005).
- [6] M. Mertz, H. Kampermann, Z. Shadman, and D. Bruß, Quantum key distribution with finite resources: Taking advantage of quantum noise, *Physical Review A—Atomic, Molecular, and Optical Physics* **87**, 042312 (2013).
- [7] B. Kraus, N. Gisin, and R. Renner, Lower and upper bounds on the secret-key rate for quantum key distribution protocols using one-way classical communication, *Physical review letters* **95**, 080501 (2005).
- [8] J. M. Renes and G. Smith, Noisy processing and distillation of private quantum states, *Physical review letters* **98**, 020502 (2007).
- [9] F. Dupuis, Privacy amplification and decoupling without smoothing, *IEEE Transactions on Information Theory* **69**, 7784 (2023).
- [10] L. Kamin, A. Arqand, I. George, N. Lütkenhaus, and E. Y.-Z. Tan, Finite-size analysis of prepare-and-measure and decoy-state quantum key distribution via entropy accumulation, *PRX Quantum* **6**, 10.1103/prxquantum.6.020342 (2025).
- [11] L. Kamin, J. Burniston, and E. Y.-Z. Tan, Rényi security framework against coherent attacks applied to decoy-state qkd, *arXiv preprint arXiv:2504.12248* (2025).
- [12] M. Navarro, A. G. Lorente, P. V. Parellada, C. Pascual-García, and M. Araújo, Finite-size quantum key distribution rates from Rényi entropies using conic optimization, *arXiv preprint arXiv:2511.10584* (2025).
- [13] G. Staffieri, G. Scala, and C. Lupo, Finite-size secret-key rates of discrete modulation continuous-variable quantum key distribution under gaussian attacks, *Physical Review A* **113**, 022445 (2026).
- [14] S. Yamano, T. Matsuura, Y. Kuramochi, T. Sasaki, and M. Koashi, General treatment of gaussian trusted noise in continuous variable quantum key distribution, *arXiv preprint arXiv:2305.17684* (2023).
- [15] I. George, J. Lin, T. van Himbeek, K. Fang, and N. Lütkenhaus, Finite-key analysis of quantum key distribution with characterized devices using entropy accumulation, *Quantum* **9**, 1941 (2025).
- [16] A. Winick, N. Lütkenhaus, and P. J. Coles, Reliable numerical key rates for quantum key distribution, *Quantum* **2**, 77 (2018).
- [17] I. George, J. Lin, and N. Lütkenhaus, Numerical calculations of the finite key rate for general quantum key distribution protocols, *Phys. Rev. Research* **3**, 013274 (2021), *arXiv:2004.11865* [quant-ph].
- [18] M. Frank, P. Wolfe, *et al.*, An algorithm for quadratic programming, *Naval research logistics quarterly* **3**, 95 (1956).
- [19] R. R. Chung, N. H. Ng, and Y. Cai, Generalized numerical framework for improved finite-sized key rates with Rényi entropy, *Physical Review A* **112**, 012612 (2025).
- [20] M. Tomamichel, M. Berta, and M. Hayashi, Relating different quantum generalizations of the conditional Rényi entropy, *Journal of Mathematical Physics* **55** (2014).
- [21] Q. Zhang, W. Zhong, M.-M. Du, S.-T. Shen, X.-Y. Li, A.-L. Zhang, L. Zhou, and Y.-B. Sheng, Device-independent quantum secret sharing with noise preprocessing and postselection, *Physical Review A* **110**, 042403 (2024).
- [22] S. A. Ghoreishi, G. Scala, R. Renner, L. L. Tacca, J. Bouda, S. P. Walborn, and M. Pawłowski, The future of secure communications: Device independence in quantum key distribution, *Physics Reports* **1149**, 1 (2025).
- [23] E. Y.-Z. Tan, P. Sekatski, J.-D. Bancal, R. Schwonnek, R. Renner, N. Sangouard, and C. C.-W. Lim, Improved DIQKD protocols with finite-size analysis, *Quantum* **6**, 880 (2022).

- [24] B. Ulu, N. Brunner, and M. Weilenmann, Device independent quantum key activation, *Physical Review Letters* **135**, 190801 (2025).
- [25] B. Regula and M. Tomamichel, Rethinking quantum smooth entropies: Tight one-shot analysis of quantum privacy amplification, arXiv preprint arXiv:2603.04493 (2026).
- [26] G. Staffieri, G. D’Ambruoso, G. Scala, and C. Lupo, Python code for analysis of finite-size bb84 protocol with trusted noise preprocessing (2026).
- [27] R. Bhatia, *Matrix analysis*, Vol. 169 (Springer Science & Business Media, 2013).
- [28] R. Rubboli and M. Tomamichel, New additivity properties of the relative entropy of entanglement and its generalizations, arXiv preprint arXiv:2211.12804 (2022).
- [29] M. Tomamichel, A framework for non-asymptotic quantum information theory, arXiv preprint arXiv:1203.2142 (2012).
- [30] P. J. Coles, Unification of different views of decoherence and discord, *Physical Review A—Atomic, Molecular, and Optical Physics* **85**, 042103 (2012).
- [31] S. Bratzik, M. Mertz, H. Kampermann, and D. Bruß, Min-entropy and quantum key distribution: Nonzero key rates for “small” numbers of signals, *Physical Review A—Atomic, Molecular, and Optical Physics* **83**, 022330 (2011).
- [32] D. Bunandar, L. C. Góvia, H. Krovi, and D. Englund, Numerical finite-key analysis of quantum key distribution, *npj Quantum Information* **6**, 104 (2020).
- [33] G. Staffieri, G. Scala, and C. Lupo, Finite-size security of qkd: comparison of three proof techniques, arXiv preprint arXiv:2601.03829 (2026).
- [34] M. Tomamichel, C. Schaffner, A. Smith, and R. Renner, Leftover hashing against quantum side information, *IEEE Transactions on Information Theory* **57**, 5524 (2011).